Additional Information	NOTICE: This is the author's version of a work that was accepted for publication in Hydrometallurgy. Changes resulting from the publishing process, such as peer review, editing, corrections, structural formatting, and other quality control mechanisms may not be reflected in this document. Changes may have been made to this work since it was submitted for publication. A definitive version was subsequently published in Hydrometallurgy, Vol. 98, Issue 1-2, (August 2009)] DOI: 10.1016/j.hydromet.2009.03.015

Leaching of a low-grade, copper-nickel sulfide ore. 3. Interactions of Cu with selected sulfide minerals

M. Maley,[1] W. van Bronswijk[1] and H.R. Watling[2*]

[1] Department of Applied Chemistry, Curtin University of Technology, GPO Box U1987, Perth, Western Australia 6845;

[2] AJ Parker Cooperative Research Centre for Integrated Hydrometallurgy Solutions, CSIRO Minerals, PO Box 7229, Karawara, Western Australia 6152

*For correspondence email Helen.Watling@csiro.au , Tel: +61 8 9334 8034, Fax: +61 8 9334 8001

Abstract

Interactions between copper ions and selected sulfide mineral concentrates were investigated in flask and column tests under conditions relevant to heap leaching in order to understand why copper recovery from a copper-nickel complex sulfide ore was significantly less than nickel recovery. Both pyrrhotite and pyrite were found to play roles in copper deposition from sulfate solutions in the range pH 1-5. The non-oxidative dissolution of pyrrhotite, previously reported to occur under acidic conditions of low oxygen availability, was also found to occur in a well-aerated system. Soluble copper reacted with the generated hydrogen sulfide to form copper sulfide, mainly covellite at pH >2.3 and its re-dissolution required acid, oxygen and a strong oxidant such as ferric ion. While significant copper also precipitated from copper sulfate solutions pH >3 in the presence of pyrite, the brochantite which was formed was readily re-dissolved at pH <3. The poor recovery of copper experienced in a test heap of copper-nickel sulfide ore was attributed to the presence of pyrrhotite and the rise in pH as the leachate percolated through the heap bed. The copper would only be recovered if acidic, oxidising conditions were restored in the heap.

Keywords: Chalcopyrite, Pyrite, Pyrrhotite, Heap leaching

1. Introduction

Heap leaching and bioleaching are low-cost technologies which contribute about 20% of annual world copper production and are practised world wide. It is not surprising, therefore, that recent high nickel prices have stimulated interest in applying heap leaching to nickel laterites and heap bioleaching to low-grade and difficult–to-process nickel sulfide ores. In the latter case, the results of bench-scale tests have been sufficiently encouraging to prompt the construction and operation of test sulfide heaps in Australia, Finland and China (Watling, 2008).

In two cases, the poor recovery of copper, compared with nickel, from complex copper-nickel ores was noted. At Talvivaara, Finland, a 17,000 tonne demonstration heap was constructed using a complex ore which contained pyrrhotite, pyrite, sphalerite, pentlandite, violarite and graphite and averaged 0.56 % Zn, 0.27% Ni, 0.14% Cu and 0.02% Co (Riekkola-Vanhanen, 2007). Recoveries were Ni 92%, Zn 82%, Co 14% and Cu 2% in 500 days. The poor copper recovery was attributed to the electrochemical properties of the ore minerals.

Similarly, in about one year of operation, copper extraction from a test heap of copper-nickel sulfide ore from the Mt Sholl deposit near Karratha, Western Australia lagged behind that of nickel by about 5-6 months, only achieving an extraction of about 50% of the contained metal in the heap, compared with about 90% for nickel (Watling et al., 2009). It was hypothesized that lack of oxygen in some parts of the heap might have caused the leach chemistry to change and some solubilised copper to be re-deposited. The reasons for the disparate recoveries of nickel and copper were subsequently investigated in column and flask leaching tests. From the results of bioleaching columns (Watling et al., 2009), it was concluded that the key factor impacting on copper recovery was pyrrhotite reactivity in acidic solutions, generating hydrogen sulfide, high iron(III) concentrations and elemental sulfur. Subsequently, in abiotic columns charged with the same ore, it was found that acidity played a key role in maximising copper recovery but that lack of column aeration impacted only slightly (Maley et al., 2009). Ancillary flask tests indicated that copper in solution was adsorbed by, or had reacted with one or more components of the ore.

In the present study, the interactions of soluble copper with the ore minerals pyrrhotite, chalcopyrite and pentlandite were investigated in flask tests under

conditions relevant to heap leaching. In addition, because it is a commonly found mineral in complex sulfide ores, the interaction of copper with pyrite was also investigated. The conditions under which the copper that was deposited on pyrite or pyrrhotite surfaces could be recovered were investigated in column tests using concentrates supported on an inert host rock. Treated residues were examined using X-ray diffraction, Raman spectroscopy and SEM-based analytical techniques to identify copper-rich insoluble species and thus assist in describing the reaction chemistry of the different systems.

2. Materials and Methods

2.1. Sulfide concentrates and copper-nickel ore

A representative sample of a copper-nickel sulfide ore from the Mt Sholl deposit near Karratha, Western Australia was pulverised to 100% passing a 125 μm screen. Mineralogical analysis using the Rietveld refinement of X-ray diffraction (XRD) data (Watling et al., 2009) revealed that the ore was comprised primarily of silicate minerals, augite (48%), amphibole (actinolite with magnesiohornblende - 24%) and chlorite (10%), with minor phases quartz and albite. The sulfide minerals were pyrrhotite (11%), chalcopyrite (2-4%), and pentlandite (1-2%).

The chalcopyrite ($CuFeS_2$) was a flotation concentrate prepared from the copper-nickel sulfide deposit at Radio Hill, Western Australia. The concentrate was comprised almost entirely of chalcopyrite with very small amounts of pentlandite.

The pentlandite ($(NiFe)_9S_8$) was a flotation concentrate also prepared from the copper-nickel sulfide deposit at Radio Hill. The concentrate contained primarily pentlandite, as well as minor quantities of chalcopyrite, pyrrhotite and small amounts of various silicates.

The pyrite (FeS_2) concentrate was provided by Kalgoorlie Consolidated Gold Mines, Western Australia, and consisted of pyrite and small amounts of quartz and other silicates.

A pyrrhotite ($Fe_{1-x}S$ where x varies from 0 to 0.125) concentrate from the Renison Bell tin mine in Tasmania, was obtained from the mineral collection at CSIRO Minerals. In this paper, pyrrhotite is shown as FeS. The concentrate

comprised hexagonal and monoclinic pyrrhotite with trace quantities of unidentified phases and quartz.

Quartz was crushed and screened to provide the inert 'host rock' that supported the concentrates for column leaching tests.

2.2. Reaction of copper with mineral sulfides (flask tests)

Copper sulfate solution (150 mL; 1 g/L Cu and selected pH) was accurately weighed into a clean, dry, sterile 250mL conical flask. The total mass of each flask and solution was recorded, and a sample of solution (~1.5 mL) was removed for analysis using a sterile Pasteur pipette. The mass of the flask and solution was recorded again. An accurately weighed amount of sulfide concentrate (~4 g, ~2.5% w/v) was added to each flask, after which the flask was weighed again. The flasks were placed in an orbital shaker (180 rpm) with the temperature controlled at 45 ^{o}C.

Loss of solution by evaporation was compensated periodically by removing the flasks from the shaker and making up their previous mass by the addition of sterile deionised water. After the addition of water the flasks were shaken thoroughly and allowed to sit for 5 min so that the solid material would settle on the bottom of the flask. A sample of solution (~1.5 mL) was removed using a sterile glass Pasteur pipette and transferred to a microcentrifuge tube. The sample was centrifuged at 16,100 rpm for 10 min, after which the supernatant solution was drawn off and its pH, redox potential and ferrous ion concentration determined. Concentrated hydrochloric acid (0.5 mL) was added to 1.0 mL of each sample and the Cu, Ni and Fe concentrations determined using inductively-coupled plasma – atomic emission spectrometry (ICP).

After sampling, the pH of each experimental solution was adjusted to the required set point using sulfuric acid. The total mass of the flask and contents after pH adjustment was recorded before returning the flask to the shaker. At the conclusion of leaching the solid residue was collected using a 0.45 μm membrane filter, and rinsed with sulfuric acid diluted to the experimental pH using deionised water. The solids were dried at ambient temperature (20-25^{o}C) to minimise oxidation of the resultant products.

The pH range tested in these experiments was pH 1 to 4, except for pyrrhotite, for which the range was pH 1 to 5.

2.3. *Dissolution of covellite using ferric ion or acid (flask tests)*

Ferric ion oxidation of covellite was examined at 45^{o}C using the procedure outlined above. In each flask, an accurately weighed sample of covellite (~3 g) was mixed with ferric sulfate solution of the selected concentration and pH (~120 mL). The selected set points were pH 1, 1.5 and 1.8. Ferric ion concentrations of approximately 2, 1 and 0.1 g/L were tested. After 239 h, an additional amount of ferric sulfate was added to each flask to restore the ferric ion concentration to its initial concentration. The acid leaching of covellite using sulfuric acid solutions in the range pH 1 to 4 was similarly investigated.

2.4. Column tests using quartz as support rock

A known mass of quartz of particle size range -13.75+4.8 mm was mixed for 10 min with an iron sulfide concentrate and 1 L sulfuric acid solution (pH 2) in a small cement mixer (Table 1). The coated quartz particles were removed from the mixer and dried at ambient temperature overnight. For each sulfide, four water-jacketed columns (500 mm height, 120 mm diameter) equipped with air inlets were charged with the dried, coated quartz. Selected columns were aerated at 1 or 3 L/min (as noted with the results). Each column was operated at 45 ^{o}C and irrigated (1 mL/min) with synthetic leach solution (8 L; pH 1.0, 1.8, 2.5 or 3.0) containing AR grade nickel sulfate (95 mg/L Ni), copper sulfate (84 mg/L Cu), ferrous sulfate (75 mg/L Fe) and the biocide sodium benzoate (C_6H_5COONa – 0.10 g/L). Solutions were recirculated through the column reservoirs. Water lost through evaporation was compensated by the addition of deionised water prior to sampling, and the solution pH in the reservoirs was adjusted by the addition of concentrated sulfuric acid post sampling. Samples of the column discharges and the reservoir solutions were collected periodically and analysed. Ferrous ion concentrations, pH and solution potentials were determined directly on the samples. Aliquots (1.0 mL) of experimental solutions were acidified with 0.5 mL concentrated hydrochloric acid solution for elemental analysis.

At the conclusion of the experiment, the columns were drained and the coated quartz particles collected. The sulfides were removed from the support rock by rinsing

with deionised water and filtration of the resulting slurry, and then dried at ambient temperature.

2.4. Analytical

Solutions were analysed for Ni, Cu and Fe using a Varian Liberty 220 ICP-AES. The plasma was located in the axial position, with a total sample uptake time of 18 s and a washout time of 15 s. Solid samples were digested in aqua regia before ICP analysis.

Solutions were analysed for ferrous ion content colorimetrically using a procedure adapted from Wilson (1960). A volume of the analyte solution (80 μL) was added to an ammonium acetate buffer containing 2,2-dipyridyl (4 mL). The absorbance of the resultant pink solution was measured at 525 nm using a Cary 50 Bio UV-vis spectrometer, with the ferrous concentration determined via a previously prepared calibration curve. Where necessary, samples were diluted quantitatively with pH 2 sulfuric acid solution before addition to the dipyridyl solution to give an absorbance within the calibration range.

X-ray powder diffraction patterns were collected from pulverised solid samples using a Philips X'Pert Automated Powder Diffractometer fitted with a Cobalt Long Line Focus X-ray tube. Patterns were collected between 2θ angles of 5-90^{o} (at 40 keV, 30 mA), and interpreted using X-plot for Windows (Version 1.34). Phases were identified using the PCPDFWIN database (Version 2.02).

Samples examined by SEM/EDS were mounted on carbon tape placed on a SEM stub and coated with two coats of carbon. The samples were analysed with a JEOL 5800LV scanning electron microscope at a working distance of 13mm. EDS analysis was performed using an Oxford Instruments Link Isis system.

Raman spectra were collected from granular solids using a Dilor LabRam 1B micro Raman spectrometer fitted with a 633nm (HeNe) laser. A diffraction grating of 1800 grooves mm^{-1} and an x 50 microscope objective were used. Spectra were acquired for 300 seconds.

3. Results and Discussion

Flask tests, initiated with similar masses of soluble copper and solid substrate were monitored for about 70 hours. Soluble copper concentrations increased to

between 1900 mg/L (pH 1.5) and 1300 mg/L (pH 4) when chalcopyrite concentrate was treated with a copper sulfate solution (initially 1 g/L Cu), but in other tests with different substrates copper remained stable (±0.02 g) or was lost from solution in increased amounts with increasing pH (Figure 1).

Direct reactions between cupric ions and chalcopyrite to form secondary copper sulfides are known, but occur very slowly (Equation 1) (Shang et al., 2001) and the oxidative leaching of chalcopyrite by oxygen or ferric ions (Equations 2 and 3) generates species that would be unlikely to remove soluble copper to a significant extent (Klauber et al., 2001; Boon and Heijnen, 1993). It is therefore unlikely that the direct reaction between cupric ions and chalcopyrite would contribute to the removal of copper species under heap leaching conditions.

$$CuFeS_2 + Cu^{2+} \rightarrow 2CuS + Fe^{2+} \quad 1$$

$$CuFeS_2 + 4Fe^{3+} \rightarrow 5Fe^{2+} + Cu^{2+} + 2S^0 \quad 2$$

$$CuFeS_2 + 4.25O_2 + H^+ \rightarrow Cu^{2+} + 2SO_4^{2-} + Fe^{3+} + 0.5H_2O \quad 3$$

Tests using pentlandite concentrate displayed a small initial increase in copper content as a portion of the small amount of copper present in the concentrate was leached (Figure 1). After this point, the amount of copper in each flask remained relatively stable with time (±0.004 g), and there was no net loss of copper during the experiment despite the increase in pH. Nickel extraction was between 10-14% in all tests.

Pentlandite is oxidised readily by both molecular oxygen and ferric ions (Equations 4 and 5) in flask tests in the relevant pH range (Southwood, 1985; Lu et al., 2000). Given that acid is consumed in the oxygen-mediated reaction (Equation 4), it is possible that localised areas of high pH, relative to the bulk solution, existed at the surface of the dissolving mineral and might have created conditions for copper reaction. However, the results indicated that reactions leading to copper loss, if they occurred, were unlikely to have contributed to the copper losses experienced in the copper-nickel ore test heap.

$$Fe_{4.5}Ni_{4.5}S_8 + 4.5O_2 + 18H^+ \rightarrow 9H_2O + 4.5Ni^{2+} + 4.5Fe^{2+} + 8S^o \quad 4$$

$$Fe_{4.5}Ni_{4.5}S_8 + 18Fe^{3+} \rightarrow 22.5Fe^{2+} + 4.5Ni^{2+} + 8S^o \quad 5$$

Pulverised ore, 100% passing a 125 μm screen, was treated with copper sulfate solution (1 g/L Cu) in the same way as the concentrates (Figure 1). At the same time, control tests at different pH (copper sulfate solutions without added ore) were conducted. There was minimal net loss of copper in the control tests (<0.004 g) confirming that solution pH alone was not the cause of copper loss. In the presence of ore, copper losses in pH 3 and pH 4 tests were substantially less than were observed for the iron sulfide concentrates, indicating that copper had reacted with a minor component of the ore rather than adsorbing onto the major silicate minerals.

Copper losses in tests using pyrrhotite and pyrite were more substantial (Figure 1), especially at high pH, and were examined in detail.

3.1. Copper deposition on pyrrhotite

All tests containing pyrrhotite experienced an initial loss of copper from solution. The decrease at pH <3 was small but significant amounts of copper were lost in the pH 4 and 5 tests (Figure 2). With the exception of the pH 1 test, the soluble copper content declined in all tests during the experiment.

Copper loss from solution appeared to be directly related to the presence of pyrrhotite, suggesting that this mineral was at least partly responsible for the delay in copper extraction in the test heap (compared with nickel recovery). No distinct trend between the amount of precipitated copper and solution pH was observed in the tests maintained at pH <3 but the quantity of copper lost increased appreciably at pH >3. Solution pH values were measured as part of the protocol to restore each solution to the desired pH set point. It was found that acid was consumed in tests with set points pH 1-3 but generated in tests with set point pH >3.

Examination of residues revealed precipitates on the pyrrhotite surfaces (Figure 3). Spot elemental analyses (SEM-EDS) gave a composition of iron, copper and sulfur but not oxygen. Elemental mapping revealed that the sulfur was mainly associated with the copper and that copper-rich locations were low in both iron and oxygen contents. If it is assumed that the iron signal originated from the underlying pyrrhotite or some iron-rich reaction products on the mineral surface, then the precipitate of interest would be a copper sulfide.

Examination of the surfaces of the untreated and the treated (pH 4) pyrrhotite using Raman spectroscopy revealed the presence of elemental sulfur and goethite, due to surface oxidation (Table 2). The diagnostic peaks for sulfur (223, 473 cm^{-1}) and goethite (250, 304, 393 cm^{-1}) species on an oxidised pyrrhotite surface have been described by Kalinkin et al. (2000). Covellite exhibits two Raman-active modes, an S-S stretch at 474 cm^{-1} and a much smaller peak at ~267 cm^{-1} from a lattice mode (Parker et al., 2003). The latter, low-intensity peak would be obscured by the more intense peaks associated with sulfur and goethite, but the covellite S-S stretch appeared to contribute to a doublet with the sulfur peak at ~470 cm^{-1}. The diagnostic peaks for copper oxide (298, 345 and 632 cm^{-1}; Reimann and Syassen, 1990) or copper hydroxy sulfates (sulfate-stretching peaks between 800-1100 cm^{-1}; Frost, 2003) were not detected in this study. Thus, on this albeit slender evidence, it was hypothesised that the copper species formed on pyrrhotite surfaces was covellite.

The residues from higher pH columns yielded very similar X-ray diffractograms. In addition to elemental sulfur and unreacted quartz, peaks associated with unreacted pyrrhotite and the iron oxyhydroxides lepidocrocite (γ-FeO(OH)) and goethite (α-FeO(OH)) were detected. Unfortunately, the expected peaks for covellite would have been obscured by some of the stronger peaks associated with goethite, lepidocrocite or sulfur, and were not distinguishable from the background noise in other parts of the diffractogram. However, by refreshing the copper solution repeatedly, quantities of reaction products were increased and, together with significant amounts of unreacted pyrrhotite, lepidocrocite and elemental sulfur, covellite and possibly trace chalcopyrite were detected in the diffractograms.

The observed results were consistent with covellite being precipitated on the pyrrhotite surface by reaction with hydrogen sulfide liberated during the non-oxidative leaching of pyrrhotite (Equation 6) (Belzile et al., 2004)). The greater extent of copper precipitation at higher pH levels was attributed to the dissociation of H_2S (Equations 7, 8) (Lide, 1995). As the pH is increased, the reactions in Equations 7 and 8 are driven to the right, increasing the concentration of the sulfide species required for the precipitation of copper sulfide (Equation 9).

$$FeS + 2H^+ \rightarrow H_2S_{(g)} + Fe^{2+} \qquad 6$$

$$H_2S \rightleftharpoons HS^- + H^+ \quad K_a = 8.9 \times 10^{-8} \qquad 7$$

$$HS^- \rightleftharpoons H^+ + S^{2-} \quad K_a = 1 \times 10^{-19} \qquad 8$$

$$S^{2-} + Cu^{2+} \rightarrow CuS \quad K_{sp} = 1 \times 10^{-44} \qquad 9$$

In respect of the trace chalcopyrite detected with the treated pyrrhotite, Cowper and Rickard (1989) reported the rapid reaction of copper ions in aqueous solution with pyrrhotite to form chalcopyrite at temperatures <100 ^{o}C and pH 2-4.5. The authors proposed a relatively complex sequential reaction pathway via several unstable intermediates. In a subsequent study, Asael et al. (2006) reported that pyrrhotite reacted with copper ions readily under anoxic conditions to form sequentially chalcopyrite, covellite and chalcocite, with covellite being the dominant phase.

3.2. Re-dissolution of copper from treated pyrrhotite

Copper behaviour in the presence of pyrrhotite was examined under conditions of aeration and limited aeration in combination with varied pH in three series of columns in which the concentrates were supported on inert quartz chips of the size typically found in a heap leach operation. The conditions were: (i) aeration and synthetic leach solution (section 2.4) at selected pH set points throughout the experiment; (ii) no aeration during copper deposition (pH 4); after deposition, synthetic leach solutions acidified to the selected pH set points and aeration applied and (iii) no aeration, initial synthetic leach solutions pH 4, acidified to the selected pH set points after copper deposition. The synthetic leach solution had a composition similar to the leachate obtained during the bioleaching of the copper-nickel sulfide ore in an agitated, aerated tank experiment.

Spraying or tumbling of a high solid density sulfide slurry onto or with an acid-stable support rock results in the formation of a thin layer of sulfide (approximately 1 mm thick) on the surface of the rock, which is stable under typical heap leach conditions (Whitlock, 1997). This procedure, known as the Geocoat™ process, was originally developed for the bacterial treatment of refractory gold ores and concentrates. However, it has also been applied successfully to the leaching of chalcopyrite concentrates in columns (Johansson et al., 1999) and is a useful research tool in the present context because the number of reactive species can be controlled.

Four columns were aerated and the synthetic leach solutions maintained at their set points between pH 1, 1.8, 2.5 and 3 throughout the experiment. These columns were intended to probe the impact of feed solution pH on copper precipitation onto pyrrhotite surfaces under well-oxygenated conditions. This experiment was similar to the operation of an aerated column loaded with ore, but effects should be magnified because the only reactive mineral present was pyrrhotite.

The copper concentrations in the four reservoirs decreased at similar rates for the first five days (Figure 4) and, for the columns with feed solutions at set points pH 2.5 and 3, continued to decrease, until almost all of the soluble copper had been removed from solution. The copper concentration in the pH 1 column reservoir decreased over a 10-day period, after which partial re-dissolution of the precipitated copper occurred as the pH continued to drop. The pH 1.8 column presented an intermediate case, with initial copper loss which then stabilized at about 30 mg/L copper in the reservoir solution.

For these columns, the pH of the discharge solutions was slightly higher than that of the feed solutions (Table 3), the total iron concentrations were strongly influenced by pH, and final copper concentrations correlated with ferric ion concentrations. For the first column, with feed solution pH 1, the start of copper re-dissolution on day 13 coincided with a drop from pH 1.7 to pH 1.4 in column discharge solution and an increase from 400 to 700 mg/L ferric ion in the reservoir solution. From this point, the discharge solution was pH $\leq$1.4 and the ferric ion concentration rose steadily. In the case of the pH 1.8 column, the discharge solution was pH >2 and the ferric ion concentration in the reservoir was <650 mg/L, throughout.

Comparison of copper curves for columns with feed solution pH 1 but different conditions of aeration (Figure 5) showed that, while aeration failed to impact on the initial copper deposition, it did impact indirectly on copper re-dissolution through its effect on ferric ion production. Ferric ion generation was low and copper re-dissolution did not occur in the unaerated column even though the discharge solution fell to and remained at pH 1.1 (data not shown, see Table 3), indicating that pH alone has little impact on copper re-dissolution.

In those columns where aeration was only applied after the feed solutions had been acidified to their selected pH set points (Figure 5), re-dissolution of precipitated copper was observed only in the pH 1 column and only after a 16-day delay. The key

parameter appeared to be the ferric ion concentration, which rose to >1000 mg/L during the "copper-delay" period. Lack of oxidant (Fe^{3+}) could be the explanation for the delayed copper recovery experienced in the test heap described previously (Watling et al., 2009).

For the unaerated columns and the columns for which aeration was applied after copper deposition, copper deposition on pyrrhotite was promoted by using an initial feed solution at pH 4. When the feed solution pH was adjusted to one of the selected pH set points, a very strong odour of hydrogen sulfide (H_2S) gas was detected from all columns and their solution reservoirs, particularly those columns with the lowest pH set points. The generation of H_2S gas (Equation 6), together with the deposition of copper in the pyrrhotite columns, was consistent with the data from the flask tests, where it was proposed that copper deposition was associated with the formation of a copper sulfide, probably covellite (Equation 9), on pyrrhotite surfaces.

The results of the experiments strongly suggested that the deposition of copper in the presence of pyrrhotite was primarily governed by the leach solution pH but that the re-dissolution of the copper required the presence of an oxidising agent. The conditions required to generate ferric ions were not met in the unaerated columns, although total iron concentrations rose considerably in the low pH column (Table 3). If the columns had been inoculated with iron oxidising organisms, the amount of air available in the reservoirs may have permitted bacterially-assisted ferric ion generation (Equation 10), sufficient to cause greater re-dissolution of copper. However, this would not be the case in poorly aerated regions of a large sulfide heap because bacterial activity is dependent upon a supply of oxygen and is also strongly influenced by pH (Plumb et al., 2008; Watling et al., 2008).

$$2Fe^{2+} + 2H^{+} + 0.5O_2 \rightarrow 2Fe^{3+} + H_2O \qquad 10$$

In ancillary flask tests it was found that covellite oxidation (Equations 11 to 12) was sensitive mainly to ferric ion concentration with lesser sensitivity to pH (Figure 6). The results were consistent with the column tests, where re-dissolution of copper only occurred when the ferric ion concentration approached 1000 mg/L and the discharge solution had pH <1.5. Acid dissolution of covellite utilising dissolved oxygen (Equation 12) (Christison, 1994) was much slower than ferric ion oxidation and was largely independent of solution pH, though a slightly increased rate was observed for the higher pH solutions (Figure 7). Ferric ion concentrations during these

tests did not exceed 50 mg/L and diminished to <10 mg/L with increased pH. The presence of sulfur in the ferric ion oxidation tests and the absence of sulfur in the acid oxidation tests as observed in X-ray diffractograms of leach residues were consistent with there being two oxidation mechanisms.

$$CuS + Fe_2(SO_4)_3 \rightarrow S^o + CuSO_4 + 2FeSO_4 \quad 11$$

$$CuS + 2O_2 \rightarrow CuSO_4 \quad 12$$

Therefore, in order to minimise the precipitation of copper in a heap containing large amounts of pyrrhotite, it is necessary to ensure that a sufficient ferric ion concentration is maintained within a heap to oxidise any precipitated copper sulfide.

It is at this point that the consideration of aeration within the heap becomes important. Although column tests performed in this study using both pulverised copper-nickel ore and pyrrhotite concentrate showed that relatively high aeration rates had little effect on the prevention of precipitation in a full-scale bioleach heap, its role is significant as a driver for copper recovery. Dissolved oxygen is required to ensure that bacterial ferrous ion oxidation occurs throughout a heap. The role of dissolved oxygen becomes even more important should a heap be inoculated primarily with sulfur oxidising bacteria, as ferric ion concentrations can only be maintained by the slower, oxygen-mediated oxidation of ferrous ions in the leach liquors.

3.3. Copper deposition on pyrite

Although the copper-nickel ore contained very little pyrite, it is a common component of many copper sulfide ores, prompting a parallel investigation of copper ion interactions with pyrite. Some copper was lost from solution at all pH set points but the amounts in tests pH ≤2 were very low (Figure 8). The largest decreases in copper content were observed in the flasks with set points pH ≥2.5. At pH 4, 75% of the copper was removed from solution. In these tests, acid was consumed continuously (and was compensated by periodic acidification to the pH set point). Whilst the pH 2.5, 3 and 4 tests were frequently adjusted to their pH set points, the actual pH rose to well above pH 4, with the latter two flasks remaining at pH >5.

Well formed, tabular crystals, indicative of slow crystal growth, were formed on the pyrite surfaces in the pH 4 test (Figure 9). Both tabular and elongated, needle-shaped crystal morphologies were observed on the surfaces of pyrite in the pH 3 test.

XRD analysis of the treated pyrite (pH 4) revealed the presence of brochantite ($CuSO_4.3Cu(OH)_2$). Excluding the elemental signature (SEM-EDS) of the underlying pyrite, the signature for the precipitate was comprised of copper, sulfur and oxygen, consistent with the XRD analysis. The Raman spectrum exhibited strong similarities to the main features of the brochantite spectrum (973, 603, 591, 496 and 473 cm^{-1}) described by Burgio and Clark (2001) for those regions not obscured by the stronger pyrite spectrum. Brochantite and its related minerals posnjakite ($CuSO_4.3Cu(OH)_2.H_2O$) and langite ($CuSO_4.3Cu(OH)_2.2H_2O$) are known to exhibit both tabular and elongated morphologies (Minceva-Stefanova and Kostov, 2002) and have similar Raman spectra at the lower frequencies (Martens et al., 2003) which would make them hard to distinguish in the present study.

Brochantite was not detected when pyrrhotite surfaces were exposed to copper sulfate solutions and did not precipitate in 'control' tests conducted over the same pH range without pyrite addition. Thus it is hypothesised that the pyrite surface played a role in brochantite formation.

The interaction of copper ions with pyrite has been examined previously. Voigt et al. (1994) reported the precipitation of a copper(II) hydroxy species (not identified) at pH 8.5 under their experimental conditions. Fitzgerald et al. (1998) found that brochantite and other basic copper sulfates formed readily at pH ≥5, conditions that prevailed in the present study despite frequent acidification to the desired pH set point. Marani et al. (1995) showed that the slow addition of base to dilute copper sulfate solutions produced either posnjakite ($CuSO_4.3Cu(OH)_2.H_2O$) or mixtures of posnjakite and brochantite, the latter being the more stable. Titration of sodium hydroxide solution into a copper sulfate solution and suspension of copper hydroxide in copper sulfate solutions had earlier indicated that the formation of brochantite occurred in two stages (Equations 13, 14) (Tanaka et al., 1991).

$$Cu^{2+} + 2OH^- \rightarrow Cu(OH)_2 \qquad 13$$

$$3Cu(OH)_{2(s)} + CuSO_4 \rightarrow CuSO_4.3Cu(OH)_2 \qquad 14$$

The results obtained in the present study indicated that the reaction of copper with pyrite in pyrite-containing ores could occur at lower pH than previously reported (pH ≥2.5) and could be as significant a cause of copper deposition as the reaction of

copper with pyrrhotite. Therefore, it is possible that copper precipitation could occur in all copper sulfide heaps for ores with significant pyrite and/or pyrrhotite contents.

3.4. Re-dissolution of copper from treated pyrite

About 70 % of the copper in synthetic leach solution (pH 4) was deposited rapidly onto pyrite concentrate in columns irrigated for 16 days (Figure 10). In the same period, the pH of the column discharge solutions, initially very high, dropped moderately fast to pH 4 and then more slowly to pH ~3-3.5 (Figure 11). In the period 11-16 days with pH ~3.5, a small amount of copper re-dissolution occurred.

After the column feed solutions had been acidified, rapid re-dissolution of copper occurred in all columns, but with clear pH dependence (Figure 10). Copper was fully recovered in eight days in the pH 1 column, the pH of the discharge solution remaining at pH ~1.2 during this period. Initially rapid copper re-dissolution in the pH 1.8 column slowed markedly after four days, despite the pH of the effluent solution continuing to decrease to pH 2.15. At the conclusion of the experiment 80% of the copper reported to the solution, indicating the need for a solution pH <2.15 for complete copper-re-dissolution. The pH 2.5 and pH 3 columns displayed similar behaviour, with their discharge solutions falling to pH ~2.3 after the initial adjustment. However, copper re-dissolution was lower (only 70-75%) and slower than for the more acidic test conditions. The rapid re-dissolution of the precipitated copper on exposure to lower solution pH was consistent with the presence of copper hydroxysulfates such as brochantite.

Iron oxy-hydroxy species such as goethite (FeOOH) have been shown to form on pyrite surfaces exposed to atmospheric oxygen and water (Cases et al., 1989; de Donato et al., 1993). While the dissolution of goethite, an acid-consuming reaction (Equation 15) occurs more readily at pH <2, goethite is soluble at pH 4 (Cornell and Schwertmann, 1998), the pH of the synthetic leach solution used to irrigate the columns initially. It is therefore probable that the initial increase in discharge solution pH from all columns, from the set point pH 4 to pH>6, is caused by the dissolution of iron oxy-hydroxy species on the pyrite surface.

$$FeOOH + 3H^{+} \rightarrow Fe^{3+} + 2H_2O \qquad 15$$

Ferric ions, which constituted about 50% of the total soluble iron, were negligible at pH ≥4 but rose sharply, subject to pH, once the feed solutions were acidified (Figure 11). The presence of ferric ions would have enhanced the oxidation of pyrite (Equation 16), generating additional acid near the mineral surface which would account for the continued slow decrease in pH.

$$FeS_2 + 14Fe^{3+} + 8H_2O \rightarrow 15Fe^{2+} + 2SO_4^{2-} + 16H^+ \quad 16$$

Thus, pyrite caused the greatest loss of copper in the high pH tests (Figure 1), an observation consistent with the formation of brochantite or related basic copper sulfates, which are known to be stable at pH >5 (e.g., Zhang et al., 2002; Robbiola et al., 2008). However, the copper hydroxysulfate species formed in the column re-dissolved readily once appropriately acidic conditions were restored. In a heap, it is anticipated that insoluble copper species associated with pyrite would be recovered through prolonged recycling of acidic leach solutions through the ore bed and copper recovery would only be delayed by the amount of time required for the acidic leaching front to move through the heap.

4. Conclusions

Poor copper recoveries during the heap (bio)leaching of pyrrhotite-rich, complex copper-nickel ores are attributed to copper ion interactions with pyrrhotite surfaces. The H_2S-producing, non-oxidative dissolution of pyrrhotite, previously reported to occur under acidic conditions of low oxygen availability, also occurs in well-aerated systems, possibly in parallel with oxidative dissolution. Soluble copper in column (or heap) leachates precipitates as copper sulfide, mainly covellite, because of its extremely small solubility product. A critical pH level for copper stability in this system is pH ~2.3; higher pH leads to precipitation and lower pH lessens precipitation and may allow some re-dissolution.

Copper sulfide re-dissolution requires low pH, oxygen and an oxidant such as ferric ion. In the absence of aeration, re-dissolution of copper precipitates from pyrrhotite surfaces cannot be achieved using leach solutions as low as pH ~1. The introduction of additional O_2 via aeration does not directly cause copper re-dissolution but does enhance pyrrhotite oxidation with the result that total iron and ferric ion concentrations increase. Copper sulfide re-dissolution only occurs when a sufficient

concentration of ferric ions is present. In this study, a ferric ion concentration of about 1 g/L was required.

Although the selected copper-nickel ore did not contain significant pyrite content, pyrite often occurs in chalcopyrite and complex copper sulfide ores that may be amenable to heap bioleaching. Significant copper loss from solution was observed when a pyrite concentrate was mixed with a copper sulfate solution in tests pH >3. In this case the precipitated copper species was brochantite, or a structurally-related species. The observed acid consumption was attributed to the dissolution of oxidised iron compounds such as goethite or lepidocrocite on the pyrite surface. The loss of copper from solution is dependant on pH, and re-dissolution occurs readily at pH <3.

Loss of copper within an acid-consuming heap leach due to brochantite formation on pyrite surfaces would only be temporary. Dissolution of copper hydroxysulfates would occur readily once the pyrite surfaces were exposed to pH <3 leachate as the acid leaching front moved downwards through the heap.

Acknowledgements

Dr A. Elliot is thanked for conducting ancillary experiments to confirm the presence of copper sulfides on pyrrhotite surfaces. M. Maley is appreciative of financial support from Curtin University of Technology through a Curtin University Postgraduate Scholarship and for part funding from Titan Resources NL. Thanks are extended to Dr Colin Hunter and Titan Resources NL for a description of the problem and for supplying the ore used in this study. The support of the Australian Government through the AJ Parker Cooperative Research Centre for Integrated Hydrometallurgy Solutions is gratefully acknowledged.

References

Asael, D., Mathews, A., Bar-Mathews, M., Halicz, L., 2006. $^{65}Cu/^{63}Cu$ fractionation during copper sulphide formation from iron sulphides in aqueous solution. Paper presented at the 16th Annual VM Goldschmidt Conference (2006). Geochimica Cosmochimica Acta 70(18) A23.

Belzile, N., Chen, Y., Cai, M., Li, Y., 2004. A review on pyrrhotite oxidation. Journal of Geochemical Exploration 84, 65-76.

Boon, M., Heijnen, J.J., 1993. Mechanisms and rate limiting steps in bioleaching of sphalerite, chalcopyrite and pyrite with *Thiobacillus ferrooxidans*. In Torma, A.E., Wey, J.L., Lakshmanan, V.L. (Eds.), Biohydrometallurgical Technologies, the Minerals, Metals & Materials Society, Warrendale, pp. 217-235.

Burgio, L., Clark, R.J.H., 2001. Library of FT-Raman spectra of pigments, minerals, pigment media and varnishes, and supplement to existing library of Raman spectra of pigments with visible excitation. Spectrochimica Acta A 57, 1491-1521.

Cases, J.M., de Donato, P., Kongolo, M., Michot, L., 1989. An infrared investigation of amylxanthate adsorption by pyrite after wet grinding at natural and acid pH. Colloids and Surfaces 36, 323-338.

Christison, P., 1994. Biological column leaching of chalcocite ore. In Recent Trends in Heap Leaching, Australasian Institute of Mining and Metallurgy, Melbourne, pp. 27-34.

Cornell, R.M., Schwertmann, U., 1998. The iron oxides: Structure, properties, reactions, occurrences and uses. Wiley-VCH, Weinheim, pp. 201-220.

Cowper, M., Rickard, D., 1989. Mechanism of chalcopyrite formation from iron monosulphides in aqueous solutions (<100 ^{o}C, pH 2-4.5). Chemical Geology 78, 325-341.

de Donato, P., Mustin, C., Benoit, R., Erre, R., 1993. Spatial distribution of iron and sulphur species on the surface of pyrite. Applied Surface Science 68, 81-93.

Fitzgerald, K.P., Nairn, J., Atrens, A., 1998. The chemistry of copper patination. Corrosion Science 40, 2029-2050.

Frost, R.L., 2003. Raman spectroscopy of selected copper minerals of significance in corrosion. Spectrochimica Acta A 59, 1195-1204.

Johansson, C., Shrader, V., Suissa, J., Autwum, K., Kohr, W., 1999. Use of the GEOCOAT^{TM} process for the recovery of copper from chalcopyrite. In Amils, R., Ballester, A. (Eds.), Biohydrometallurgy and the Environment Toward the Mining of the 21st Century Part A, Elsevier, Amsterdam, pp. 569-576.

Kalinkin, A.M., Forsling, W., Makarov, D.V., Makarov, V.N., 2000. Surface oxidation of synthetic pyrrhotite during wetting-drying treatment. Environmental Engineering Science 17, 329-335.

Klauber, C., Parker, A., van Bronswijk, W., Watling, H., 2001. Sulphur speciation of leached chalcopyrite surfaces as determined by X-ray photoelectron spectroscopy. International Journal of Mineral Processing 62, 65-94.

Lide, D.R., 1995. CRC Handbook of Chemistry and Physics 75th edition. CRC Press, Boca Raton, p. **8**-43.

Lu, Z.Y., Jeffrey, M.I., Zhu, Y., Lawson, F., 2000. Studies of pentlandite leaching in mixed oxygenated acidic chloride-sulfate solutions. Hydrometallurgy 56, 63-74.

Maley M., van Bronswijk, W., Watling, H.R., 2009. Leaching of a low-grade, copper-nickel sulfide ore. 2. Impact of aeration and pH on Cu recovery during abiotic leaching. Hydrometallurgy (submitted).

Marani D., Patterson, J.W., Anderson, P.R., 1995. Alkaline precipitation and aging of Cu(II) in the presence of sulfate. Water Research 29, 1317-1326.

Martens, W., Frost, R.L., Kloprogge, J.T., Williams, P.A., 2003. Raman spectroscopic study of the basic copper sulphates – implications for copper corrosion and 'bronze disease'. Journal of Raman Spectroscopy 34, 145-151.

Minceva-Stefanova, J., Kostov, I., 2002. Morphology vs. Structure of langite and posnjakite. Comptes rendus de l'Academie Bulgare des Sciences 55, 57-60.

Parker, G., Woods, R., Hope, G., 2003. Raman investigation of sulfide leaching. In Young, C.A., Alfantazi, A.M., Anderson, C.G., Dreisinger, D.B., Harris, B., James, A. (Eds.), Hydrometallurgy 2003 (Vancouver), Volume 1, Leaching and solution purification, TMS, Warrendale, pp. 447-460.

Plumb, J.J., Muddle, R., Franzmann, P.D., 2008. Effect of pH on rates of iron and sulfur oxidation by bioleaching organisms. Minerals Engineering 21, 76-82.

Reimann, K., Syassen, K., 1990. Pressure dependence of Raman modes in CuO. Solid State Communications 75, 137-140.

Riekkola-Vanhanen, M., 2007. Talvivaara black schist bioheapleaching demonstration plant. Advanced Materials Research 20-21, 30-33.

Robbiola, L., Rahmouni, K., Chiavari, C., Martini, C., Prandstraller, D., Texier, A., Takenouti, H., Vermaut, P., 2008. New insight into the nature and properties of pale green surfaces of outdoor bronze monuments. Applied Physics A. Materials Science & Processing 92, 161-169.

Shang, C., Lin, W., Liu, C., 2001. A simulation of the supergene copper enrichment process. Proceedings of the National Science Council ROC(A) 25, 293-299.

Southwood, M.J., 1985. The acid leaching of nickel and copper from sulphidic ore in the presence of pyrite. Journal of the South African Institute of Mining and Metallurgy 85, 395-401.

Tanaka, H., Kawano, M., Koga, N., 1991. Thermogravimetry of basic copper sulphates obtained by titrating NaOH solution with $CuSO_4$ solution. Thermochimica Acta 182, 281-292.

Voigt, S., Szargan, R., Suoninen, E., 1994. Interaction of copper(II) ions with pyrite and its influence on ethyl xanthate adsorption. Surface and Interface Science 21, 526-536.

Watling, H.R., 2008. The bioleaching of nickel-copper sulfides. Hydrometallurgy, 91, 70-88.

Watling, H.R., Elliot, A.D., Maley, M., van Bronswijk, W., Hunter, C., 2009. Leaching of a low-grade, copper-nickel sulfide ore. 1. Impact of acid pre-conditioning, inoculation and aeration on Cu recovery during column bioleaching. Hydrometallurgy (submitted)

Watling, H.R., Perrot, F.E., Shiers, D.W., 2008. Comparison of selected characteristics of *Sulfobacillus* species and review of their occurrence in acidic and bioleaching environments. Hydrometallurgy 93, 57-65.

Whitlock, J.L., Biooxidation of refractory gold ores (The Geobiotics Process). In Rawlings, D.E. (Ed.), Biomining: Theory, Microbes and Industrial Processes. Springer, New York, pp. 117-127.

Wilson, A.D., 1960. The micro determination of ferrous iron in silicate minerals by a volumetric and colorimetric method. Analyst 85, 823-827.

Zhang, X.Y., He, W.L., Wallinder, I.O., Pan, J., Leygraf, C., 2002. Determination of instantaneous corrosion rates of copper from naturally patinated copper during continuous rain events. Corrosion Science 44, 2131-2151.

Table 1. Masses of quartz and pyrite or pyrrhotite used to prepare the coated quartz particles, and the mass of 'ore' loaded into each column.

	Pyrite	Pyrrhotite	Pyrrhotite*
Mass quartz in mixture before loading (kg)	28.0	20.0	18.8
Mass sulfide in mixture before loading (kg)	3.00	1.75	1.65
Mass quartz/sulfide mixture per column (kg)	5.00	5.00	5.11
Mass iron sulfide in each column (g)	484	402	380

* Experiment: combined effect of pH and aeration on copper interaction with pyrrhotite

Table 2. Assignment of the Raman spectrum of an oxidised pyrrhotite and a copper-treated pyrrhotite obtained in this study

Pyrrhotite - observed (cm^{-1})	**Copper-treated pyrrhotite - observed (cm^{-1})**	**Assignment**
222	222	Sulfur
234	234	Goethite
287	287	Goethite
400	400	Goethite
479	~473 (doublet)	Sulfur
	~475 (doublet)	Covellite

Table 3. Final solution parameters after pyrrhotite column operation

Feed solution pH set point	Discharge solution pH	Cu mg/L	Fe mg/L	Fe^{3+} mg/L
Aerated columns (1 L/min), feed solutions at pH set point, 25 days operation				
1	1.2	51	9050	2580
1.8	2.2	25	2010	610
2.5	3.0	7	1160	130
3	3.8	1	1110	<100
Feed solution pH 4 initially; pH adjusted and aerated (3 L/min) from day 24; 62 days operation				
1	1.1	75	14000	3680
1.8	2.5	4	3470	190
2.5	2.9	1	1200	230
3	3.3	1	1010	210
No aeration, feed solution pH 4 initially; pH adjusted day 17; 24 days operation				
1	1.1	1	15850	800
1.8	4.0	2	1690	300
2.5	3.9	1	1130	<100
3	4.1	1	1060	<100

Figure captions

Figure 1. Copper-balance results (flask tests, 45°C) from the treatment of sulfide concentrates and ore with copper sulfate solution (1 g/L Cu) at different pH set points.

Figure 2. Concentration of copper in flask tests (45°C) containing pyrrhotite concentrate and copper sulfate solution (initially 1 g/L Cu) at different pH set points. ◆ pH 1; ■ pH1.5; ▲ pH 1.8; ◊ pH 2.5; □ pH 3; △ pH 4; X pH 5.

Figure 3. SEM secondary electron image (20 keV) of precipitates formed on a pyrrhotite surface treated with copper sulfate solution (1 g/L Cu, pH 4, 45°C) during flask tests.

Figure 4. Copper concentrations in reservoir solutions for four aerated columns charged with pyrrhotite concentrate with quartz support, with feed solutions ◊ pH 1, □ pH 1.8, △pH 2.5, and ○ pH 3.

Figure 5. Copper and ferric ion concentrations in reservoir solutions. (i) an aerated column with feed solution pH 1 throughout the experiment: ◊ Cu and ∗ Fe^{3+}; (ii) a column for which the feed solution was adjusted to pH 1 and aeration was applied from day 24: ▲ Cu and ● Fe^{3+} before and △ Cu and ○ Fe^{3+} after aeration was applied.

Figure 6. Copper extraction (%) during covellite oxidation by ferric ion in acidic solutions of different pH at 45 °C (data from day 13).

Figure 8. Concentration of copper in tests containing pyrite concentrate and copper sulfate solution (1 g/L Cu, 45°C) at different pH set points. ◆ pH 1; ■ pH1.5; ▲ pH 1.8; ◊ pH 2.5; □ pH 3; △ pH 4.

Figure 9. SEM secondary electron image (20 keV, x 2500) of precipitates on a pyrite surface treated with copper sulfate solution (1 g/L Cu, pH 4, 45^{o}C).

Figure 10. Copper concentrations in reservoir solutions during copper precipitation at pH 4 (closed symbols) in the presence of pyrite and copper re-dissolution at varied pH (open symbols): ◊pH 1; □ pH 1.8; △ pH 2.5.

Figure 11. Column discharge solution pH (open symbols) and ferric ion concentrations (closed symbols) in reservoir solutions during copper treatment of pyrite. ◊pH 1; □ pH 1.8; △ pH 2.5; ○ pH 3. Reservoir solutions were acidified to their respective set points at day 16.

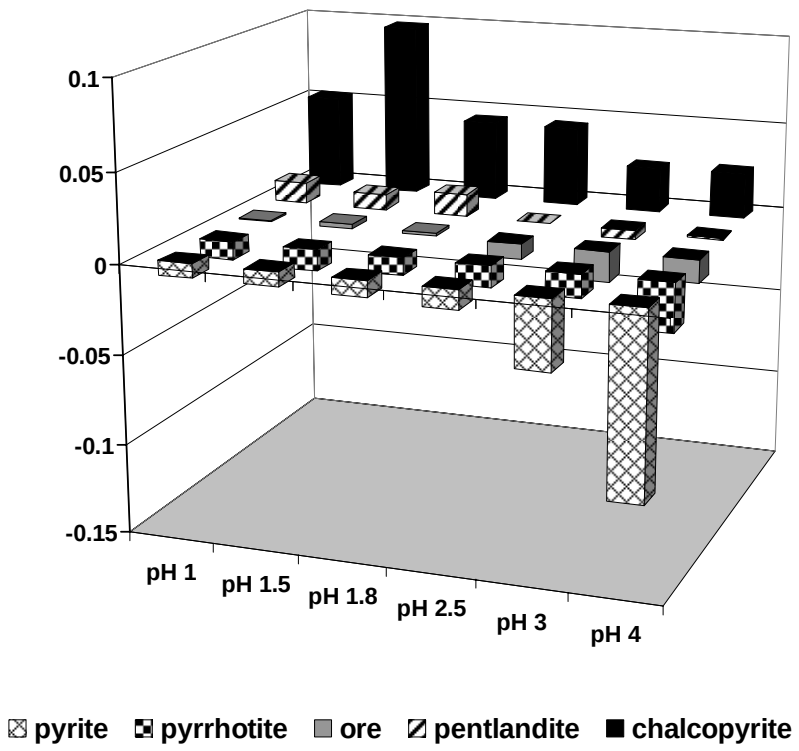

Figure 1. Copper-balance results (flask tests, 45°C) from the treatment of sulfide concentrates and ore with copper sulfate solution (1 g/L Cu) at different pH set points.

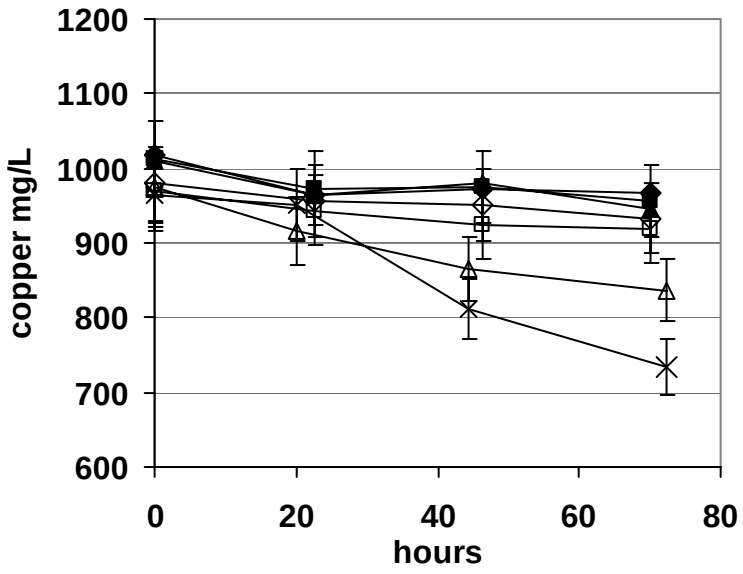

Figure 2. Concentration of copper in flask tests (45°C) containing pyrrhotite concentrate and copper sulfate solution (initially 1 g/L Cu) at different pH set points. ◆ pH 1; ■ pH1.5; ▲ pH 1.8; ◊ pH 2.5; □ pH 3; △ pH 4; X pH 5.

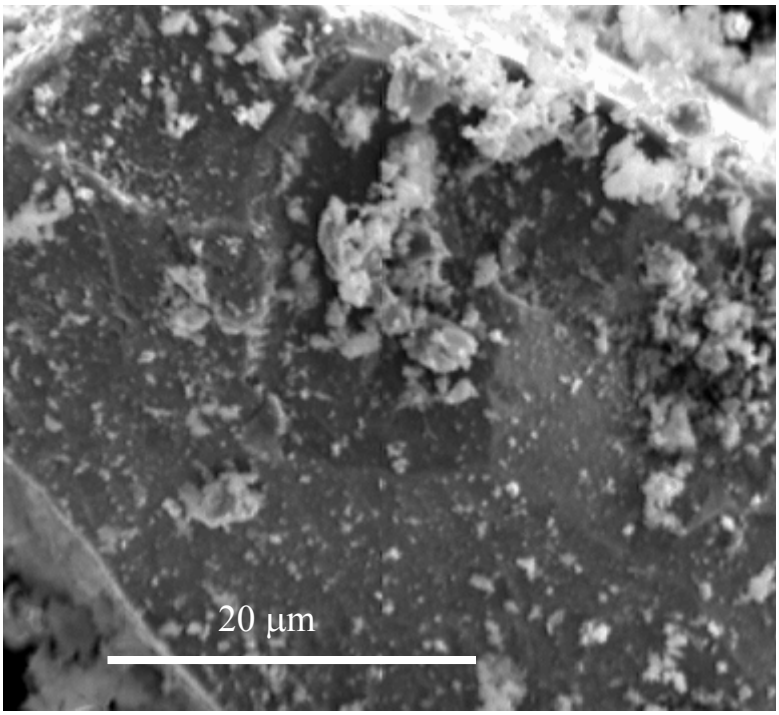

Figure 3. SEM secondary electron image (20 keV) of precipitates formed on a pyrrhotite surface treated with copper sulfate solution (1 g/L Cu; pH 4) during flask tests.

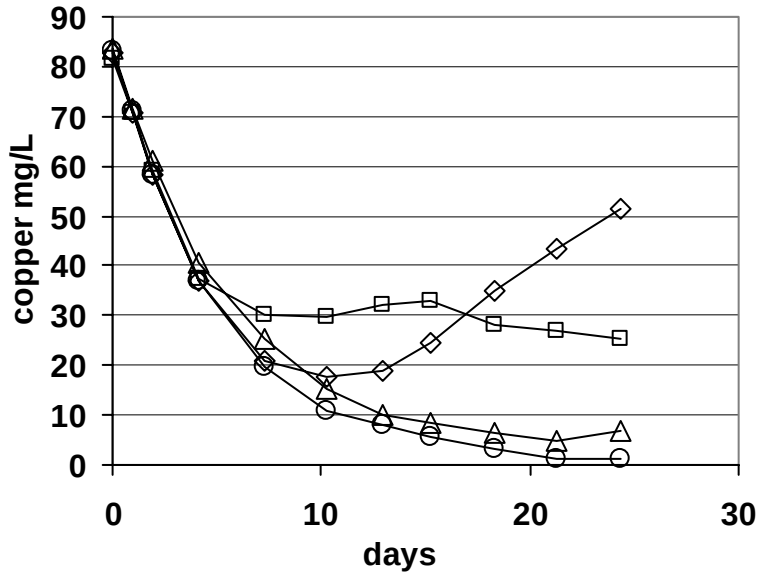

Figure 4. Copper concentrations in reservoir solutions for four aerated columns charged with pyrrhotite concentrate with quartz support, with feed solutions ♢ pH 1, □ pH 1.8, △pH 2.5, and ○ pH 3.

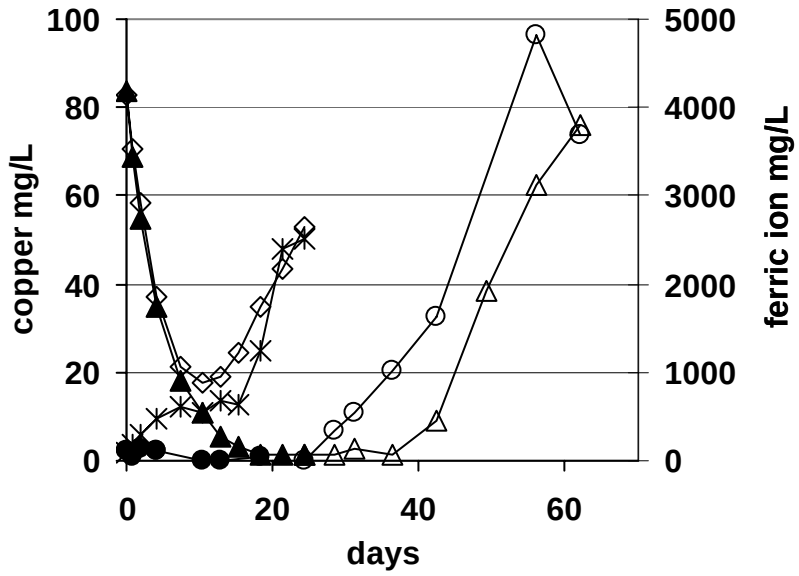

Figure 5. Copper and ferric ion concentrations in reservoir solutions. (i) an aerated column with feed solution pH 1 throughout the experiment: ◊ Cu and ∗ Fe^{3+}; (ii) a column for which the feed solution was adjusted to pH 1 and aeration was applied from day 24: ▲ Cu and ● Fe^{3+} before and △ Cu and ○ Fe^{3+} after aeration was applied.

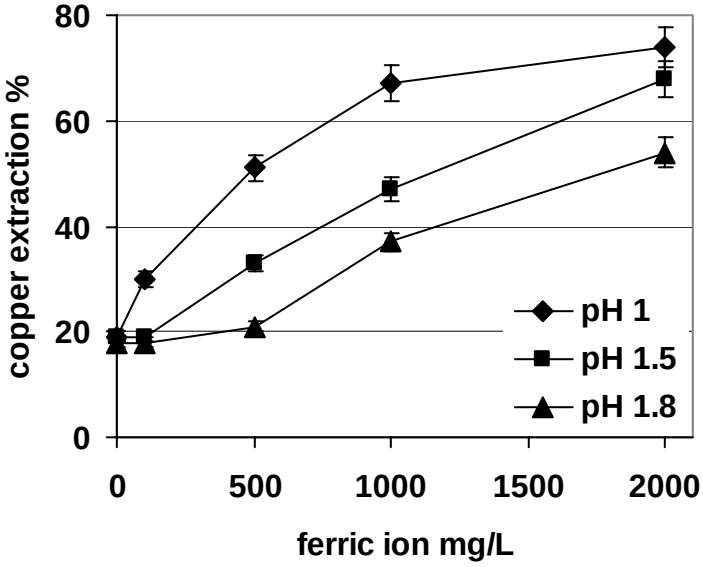

Figure 6. Copper extraction (%) during covellite oxidation by ferric ion in acidic solutions of different pH at 45 ^{o}C (data from day 13).

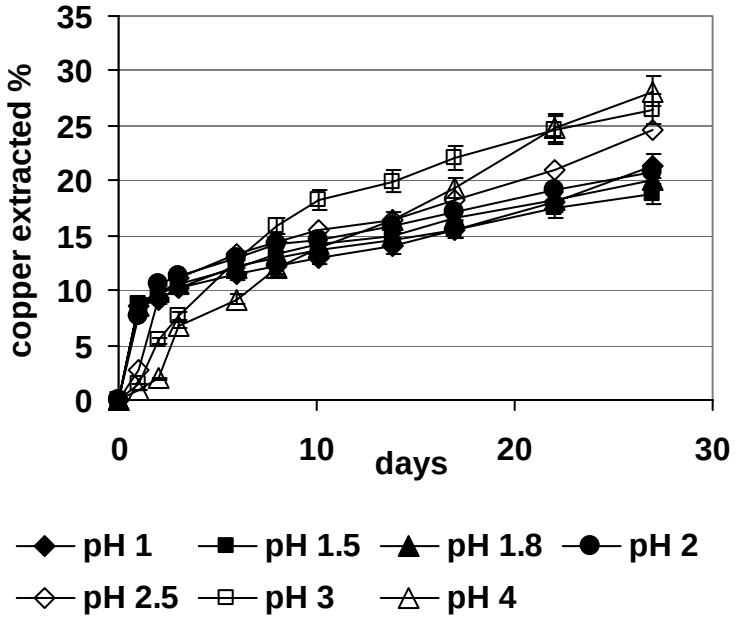

Figure 7. Copper extraction (%) during covellite oxidation in acidic solutions of different pH at 45^{o}C as a function of pH.

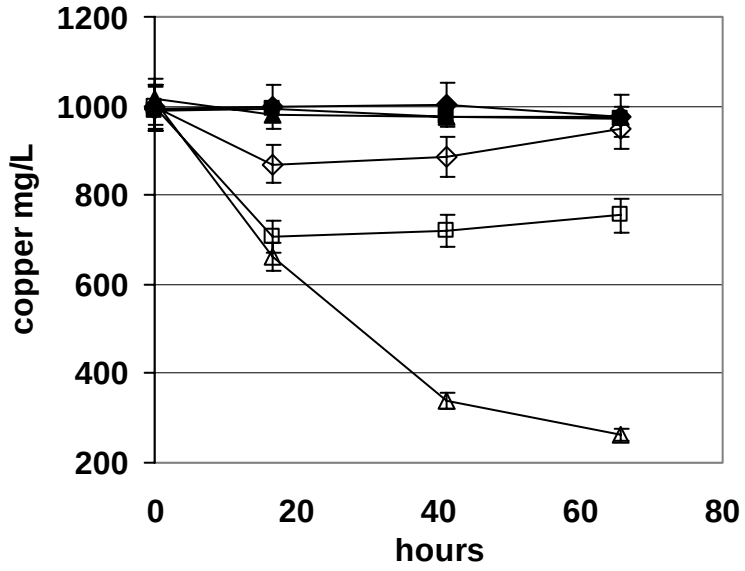

Figure 8. Concentration of copper in tests containing pyrite concentrate and copper sulfate solution (1 g/L Cu) at different pH set points. ◆ pH 1; ■ pH1.5; ▲ pH 1.8; ◊ pH 2.5; □ pH 3; △ pH 4.

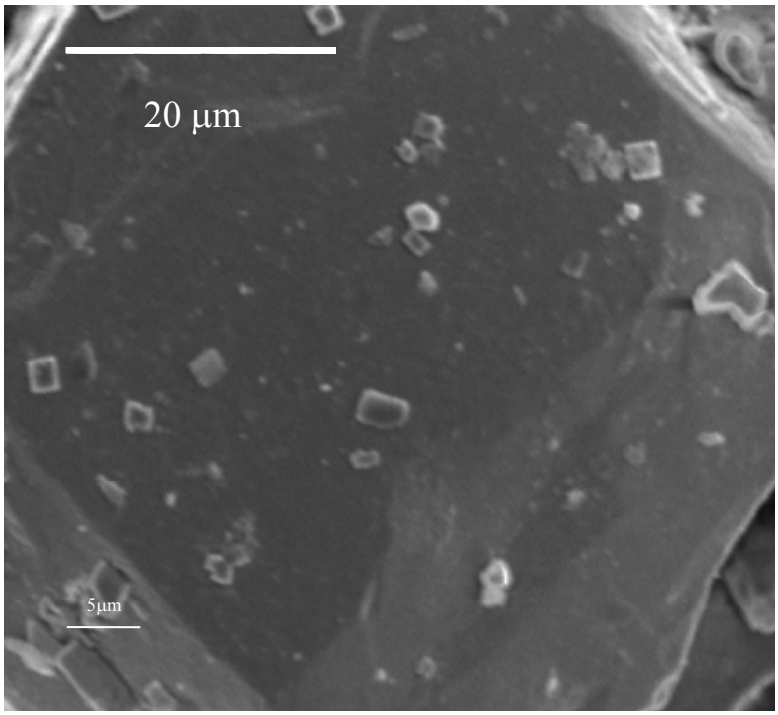

Figure 9. SEM secondary electron image (20 keV, x 2500) of precipitates on a pyrite surface treated with copper sulfate solution (1 g/L Cu; pH 4).

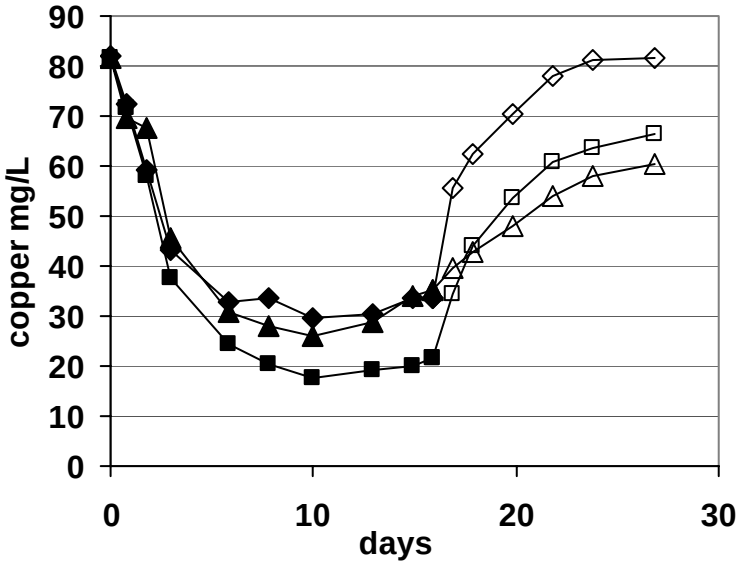

Figure 10. Copper concentrations in reservoir solutions during copper precipitation at pH 4 (closed symbols) in the presence of pyrite and copper re-dissolution at varied pH (open symbols): ◊pH 1; □ pH 1.8; △ pH 2.5.

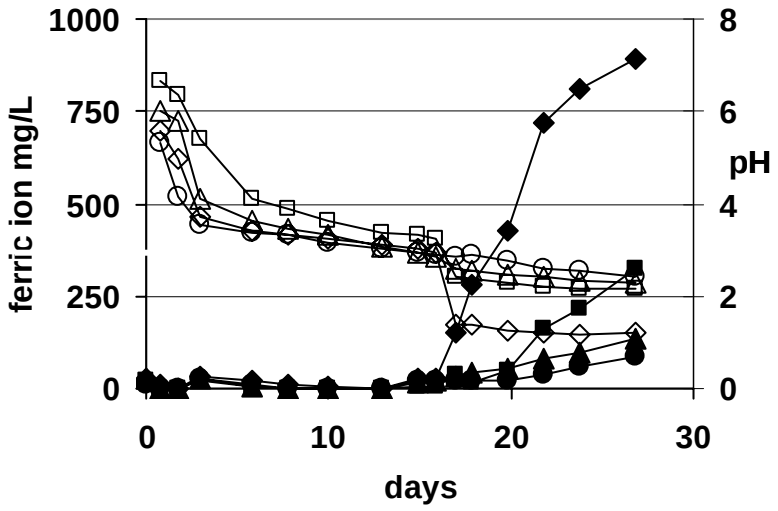

Figure 11. Column discharge solution pH (open symbols) and ferric ion concentrations (closed symbols) in reservoir solutions during copper treatment of pyrite. ◊pH 1; □ pH 1.8; △ pH 2.5; ○ pH 3. Reservoir solutions were acidified to their respective set points at day 16.